0026-895X/04/6605-1201–1212$20.00
MOLECULAR PHARMACOLOGY
Copyright © 2004 The American Society for Pharmacology and Experimental Therapeutics
Mol Pharmacol 66:1201–1212, 2004

Vol. 66, No. 5
1743/1180223
Printed in U.S.A.

The Low-Potency, Voltage-Dependent HERG Blocker Propafenone—Molecular Determinants and Drug Trapping

Harry J. Witchel, Christopher E. Dempsey, Richard B. Sessions, Matthew Perry, James T. Milnes, Jules C. Hancox, and John S. Mitcheson

Cardiovascular Research Laboratories and Department of Physiology, (H.J.W., J.T.M., J.C.H.) and Molecular Recognition Centre, Department of Biochemistry (C.E.D., R.B.S.), School of Medical Sciences, University of Bristol, Bristol, United Kingdom; and Department of Cell Physiology & Pharmacology, Medical Sciences Building, Leicester University, Leicester, United Kingdom (M.P., J.S.M.)

Received April 23, 2004; accepted August 11, 2004

ABSTRACT

The molecular determinants of high-affinity human *ether-a-go-go*-related gene (HERG) potassium channel blockade by methanesulfonanilides include two aromatic residues (Phe656 and Tyr652) on the inner helices (S6) and residues on the pore helices that face into the inner cavity, but determinants for lower-affinity HERG blockers may be different. In this study, alanine-substituted HERG channel mutants of inner cavity residues were expressed in *Xenopus laevis* oocytes and were used to characterize the HERG channel binding site of the antiarrhythmic propafenone. Propafenone's blockade of HERG was strongly dependent on residue Phe656 but was insensitive or weakly sensitive to mutation of Tyr652, Thr623, Ser624, Val625, Gly648, or Val659 and did not require functional inactivation. Homology models of HERG based on KcsA and MthK crystal structures, representing the closed and open forms of the channel, respectively, suggest propafenone is trapped in the inner cavity and is unable to interact exclusively with Phe656 in the closed state (whereas exclusive interactions between propafenone and Phe656 are found in the open-channel model). These findings are supported by very slow recovery of wild-type HERG channels from block at −120 mV, but extremely rapid recovery of D540K channels that reopen at this potential. The experiments and modeling suggest that the open-state propafenone binding-site may be formed by the Phe656 residues alone. The binding site for propafenone (which may involve π-stacking interactions with two or more Phe656 side-chains) is either perturbed or becomes less accessible because of closed-channel gating. This provides further evidence for the existence of gating-induced changes in the spatial location of Phe656 side chains.

Pharmacological blockade of the cardiac 'rapid' delayed rectifier potassium (K^+) current (I_{Kr}) is commonly associated with a drug's propensity to cause acquired long QT syndrome (Roden et al., 1996). The α-subunit of the I_{Kr} channel is encoded by *HERG* (Sanguinetti et al., 1995). Molecular determinants of this channel's blockade by the archetypal high-potency HERG blockers, the methanesulfonanilides, reside in the inner cavity of the channel pore and are composed of amino acid residues in the H5 loop (adjacent to the selectivity filter) and the S6 transmembrane domain (Lees-Miller et al., 2000; Mitcheson et al., 2000a). For all drugs tested, the molecular determinants include the amino acid residues Phe656 and Tyr652 [except for vesnarinone, which does not require Tyr652 (Kamiya et al., 2001), and fluvoxamine, which can block HERG when Phe656 or Tyr652 are mutated (Milnes et al., 2003)], and in many cases the molecular determinants additionally include a combination of Thr623, Ser624, Val625, Gly648, and Val659. Most drugs with a high-affinity for HERG have been shown to have an open-state-dependent blockade mechanism (Spector et al., 1996). Open-state blockade of HERG may involve drug trapping [e.g., MK-499 (Mitcheson et al., 2000b)], a 'foot in the door' type mechanism [e.g., chloroquine (Sanchez-Chapula et al., 2002)], or rapid unbinding upon repolarization (e.g., vesnarinone (Kamiya et al., 2001)); these different mechanisms can often be differentiated by the kinetics of current decay during deactivation.

This work was supported by project grant PG/2001104 from the British Heart Foundation (to H. J. W. and J. L. H.) and a Medical Research Council career establishment award (to J.S.M.).

This work has previously been presented in abstract form (Witchel HJ, Perry M, Milnes JT, Hancox JC, and Mitcheson JS (2003). Molecular determinants of HERG blockade by propafenone—drug trapping of a low potency voltage-dependent HERG blocker. *Biophys J* **84:**2660.).

Article, publication date, and citation information can be found at http://molpharm.aspetjournals.org.

doi:10.1124/mol.104.001743.

ABBREVIATIONS: I_{Kr}, the 'rapid' delayed rectifier potassium current; *HERG*, human *ether-à-go-go*–related gene; MK-499, (+)-*N*-[1′-(6-cyano-1,2,3,4-tetrahydro-2(*R*)-naphthalenyl)-3,4-dihydro-4(*R*)-hydroxyspiro(2*H*-1-benzopyran-2,4′-piperidin)-6-yl]methanesulfonamide; MES, 2-(*N*-morpholino)ethanesulfonic acid.

The class Ic antiarrhythmic drug propafenone (Funck-Brentano et al., 1990) can cause QT prolongation and proarrhythmia (Rehnqvist et al., 1984; Hii et al., 1991). We and others have previously shown that propafenone blocks native I_{Kr} and HERG with an open-state-dependent mechanism (Duan et al., 1993; Delpon et al., 1995; Mergenthaler et al., 2001; Paul et al., 2002), although at a substantially lower potency than methanesulfonanilides block HERG. The goal of this study was to determine how open-state-dependent blockade occurred with this drug; in particular, whether the low-affinity blockade by propafenone shared mechanistic traits of the high-affinity blockade by methanesulfonanilides at two levels: molecular determinants and drug trapping. This report demonstrates that the voltage-dependent, low-affinity blockade of HERG by propafenone deviates from that described previously for chloroquine (Sanchez-Chapula et al., 2002), and the molecular mechanism also differs from previous observations for high-affinity blockers. This finding led to the question of whether existing structural models of HERG channel blockade were sufficient to describe the block by propafenone. Therefore, an *in silico* model of HERG channel blockade in the open state was then developed, and docking simulations were performed. Comparison of the results from the computer simulations using our new open-channel model with those using a closed-channel model lead us to propose an alternative open-channel blocking mechanism. This mechanism incorporates drug trapping in the closed state and strong interactions with Phe656 in the open state of the channel.

Materials and Methods

Measurements of Heterologous HERG Currents. Isolation of *Xenopus laevis* oocytes, their handling and injection with mRNA, creation of mutant channel cDNAs, and two-electrode voltage clamp with rapid solution switching was performed as described previously (Mitcheson et al., 2000a,b). Capped RNA from linear template DNA was made using the mMessage mMachine kit, and between 5 and 30 ng of RNA was injected into each oocyte and allowed to express between 1 and 4 days before making recordings. The electrode solution was 3 M KCl. The extracellular recording solution was low in Cl^- (which was substituted for by MES) and consisted of 96 mM NaMES, 2 mM KMES, 2 mM $CaMES_2$, 5 mM HEPES, and 1 mM $MgCl_2$, adjusted to pH 7.6 with MES (Mitcheson et al., 2000a,b). Substitution of chloride by MES results in substantially reduced endogenous chloride currents (see Fig. 5 in Mergenthaler et al., 2001). Some mutants (e.g., T623A and G648A) have a left-shifted voltage dependence of inactivation and do not conduct current under standard recording conditions. These mutants were investigated using a "high-K^+" extracellular superfusate containing 96 mM K^+ and 2 mM Na^+. Propafenone (Sigma, St. Louis, MO) was dissolved directly in extracellular recording solutions by heating briefly to 70°C.

The voltage command protocols (applied at room temperature) used for determining molecular determinants of blockade were: all cells held at −90 mV, then a 2-s step to 0 mV, followed by observation of tails for 2 s at −70 mV for wild-type HERG and most mutants (interpulse interval 10 s). For F656A and V659A, tail currents were observed at −140 mV, and V625A tail currents were observed at −90 mV. For most experiments, the response to propafenone was quantified from measurements of peak tail current amplitude. S631A and G628C/S631C block were quantified from isochronal 'end pulse' currents, which were larger than the tail currents (results derived from S631A tail currents and S631A end pulse currents were very similar—G628C/S631C tail currents were too small to measure).

Steady-state HERG current baselines were attained by repetitively pulsing to 0 mV (100–200 sweeps). A constant flow of superfusate was applied with a 'rapid solution switcher' (adapted for oocytes from Levi et al., 1996). Initial application of propafenone always began with exposure to the drug for 2 min while maintaining the holding potential of the oocytes at −90 mV. Initial blockade invariably occurred in less than 200 ms during the first sweep at 0 mV; this type of blockade we have called "pseudo-steady-state" because block increased very slowly thereafter. Recovery from pseudo-steady-state block did not occur in closed-channels but could be induced after washing out the bath with control solution for 5 min and opening channels by a prolonged depolarization. Steady-state drug blockade resulted from more prolonged exposure to propafenone accompanied by extensive pulsing (>75 sweeps), and the potency of steady state blockade was slightly greater than that of pseudo-steady-state blockade. Steady-state block was only slightly reversible. The difference between steady-state and pseudo-steady-state block may possibly involve drug accumulation intracellularly and binding associated with the lipophilic yolk sac of the oocyte. All the experiments on the molecular determinants of blockade were performed using steady-state block; experiments on drug trapping were done using pseudo-steady-state block. IC_{50} values for propafenone were determined by fitting the concentration response data with the Hill function $Y = 1/[1 + 10^{(\mathrm{LogIC_{50}} - X) \times n_H}]$ (Prism, GraphPad Software Inc., San Diego CA), where X is the logarithm of concentration and Y is the blockade; maximum and minimum values for the blockade were fixed at 1 and 0 at points 3 orders of magnitude from the observed maxima and minima. Values for IC_{50} were calculated with 95% confidence intervals; all other statistical measures are presented as mean ± S.E.M.

Computer Modeling. HERG pore homology models were constructed based on sequence homology with the pore regions of KcsA (closed-pore model) and MthK (open-pore model) and using as templates the X-ray crystal structures determined previously (Doyle et al., 1998; Jiang et al., 2002) (Protein Data Bank accession codes: KcsA, 1BL8; MthK, 1LNQ). Only the sequence corresponding to the selectivity filter, pore helix, and S6 helix were modeled, because this region provides all the residues that comprise the pore and because the homologies of S5 of HERG with the outer transmembrane helices of KcsA and MthK are not fully defined.

Homology models were constructed within the Biopolymer and Builder modules of InsightII (Accelrys, San Diego, CA) by "mutating" the amino acids of KcsA or MthK to the corresponding amino acids of HERG. For the closed-pore model, side-chain rotamers were chosen to match the rotamers of KcsA up to the side-chain β atoms, where relevant. Because the MthK crystal structure contains backbone coordinates only, the side-chain rotamers were introduced according to the most highly populated rotamer in the crystal structure database for the relevant secondary structure type. Each model was visually inspected, and selecting the side-chain rotamer that gave the lowest energy relieved severe spatial clashes of amino acid side chains. Finally, each model was energy-minimized by 2000 steps of steepest descents using Discover. The structures of both stereoisomers of propafenone were constructed within InsightII and energy minimized. Because the tertiary amino group has a pK_a of 8.8, this amino group was maintained in its protonated (charged) form. The two stereoisomers of MK-499 were also constructed (positively charged secondary amino group) for docking runs for comparison with structures produced previously (Mitcheson et al., 2000a). This provides a check on the extent to which separate docking algorithms and different homology models produce a coherent picture for docking of this drug into the closed-pore HERG model. We found that the lowest energy structures of MK-499 bound to our closed-channel homology model were generally similar to those described previously (Mitcheson et al., 2000a) for binding of MK-499 to a KcsA-based closed-channel homology model using flexible ligands oriented on grid (FLOG) docking methods (not shown).

Docking runs were performed using FlexiDock within Sybyl 6.9. FlexiDock uses a genetic algorithm to explore the conformational and orientational space that defines possible interactions between the ligand and its binding site. The program requires initial place-

ment of the ligand into a potential binding site, the latter being defined as the amino acids selected together with any atoms within 4.5 Å. FlexiDock allows selected bonds in both the ligand and binding site to be rotated during sampling of conformational space. Based on the mutagenesis data, the binding site for propafenone is within the pore and incorporates interactions with Phe656. However, to avoid bias in the modeling, the binding site in most runs included most of the amino acid side chains on the S6 helix that project into the pore in closed-state models. These are Gly648, Ser649, Tyr652, Phe656, and Ser660. In some runs, the residues facing the inner cavity of the pore below the selectivity filter (Thr623, Ser624, and Val625) were also included. All possible rotatable bonds within the ligands were selected, and all rotatable bonds in the side chains that define the potential binding site were selected (excluding trivial bond rotations involving X-H bonds).

For the propafenone-HERG models presented here, at least 20 FlexiDock runs were made with different starting positions and orientations of the ligand within either the open- or closed-state models. In general, runs with 20,000 generations within the genetic algorithm were made to obtain a series of 6 to 12 different low-energy structures. These were used as starting points for longer (80,000–120,000 generation) runs, which normally gave high levels of convergence (70–80%), indicating that the lowest energy structure within the particular set of minima explored in that run had been achieved. Approximately 4,000,000 FlexiDock generations were sampled for propafenone binding to each of the open- and closed-channel models (Table 1).

Results

S6 Inner Helix Mutations and Their Effects on Propafenone Mediated Blockade. To determine whether the molecular determinants of blockade of HERG by propafenone were similar to those described previously in the S6 inner helix, as observed with other drugs (Mitcheson et al., 2000a), channels having mutations of residues modeled to line the inner cavity and selectivity filter were tested for functional drug blockade; the testing of these mutants does not exclude the possibility that additional binding interactions might occur for S5 residues and other S6 residues thought not to line the pore (Ishii et al., 2001; Gessner et al., 2004).

A propafenone concentration (50 μM) causing profound blockade of wild-type HERG current (I_{HERG}) was used to test HERG channel mutants (Fig. 1). It inhibited wild-type I_{HERG} tails at −70 mV by 96.4 ± 0.1% (mean ± S.E.M., 2 mM $[K^+]_o$; $n = 5$), and at −140 mV by 79.6 ± 4.9% (2 mM $[K^+]_o$; $n = 5$). With raised $[K^+]_o$ (96 mM), wild-type I_{HERG} tails at −70 mV were inhibited by 88.3 ± 2.5% ($n = 5$). Propafenone (50 μM) blocked the mutant HERG channel F656A by only 5.0 ± 9.7% ($n = 5$), demonstrating that, as for the methanesulfonanilides, dofetilide, and MK-499 (Lees-Miller et al., 2000; Mitcheson et al., 2000a), the Phe656 residue is a critical determinant of HERG channel blockade for propafenone. To estimate the order of magnitude of attenuation, we also tested 100 and 300 μM propafenone, which blocked F656A by 22.6 ± 8.8% and 66.4 ± 2.6%, respectively ($n = 5$); higher concentrations of propafenone were difficult to solubilize, but fitting the three concentrations tested to a Hill plot led to an estimate of an IC_{50} ~ 100-fold higher than wild-type HERG (Table 2). This shift is similar to values seen with F656A for cisapride and terfenadine (Mitcheson et al., 2000a). Phe656 has also been shown to be a molecular determinant for the other class I antiarrhythmic tested, quinidine (Lees-Miller et al., 2000); quinidine blocks wild-type HERG at a potency similar to that of propafenone when measured under similar conditions (Paul et al., 2002).

In contrast, for all other mutations tested [located in either the pore helix or S6 regions, and selected on the basis of being molecular determinants for those agents previously studied (Mitcheson et al., 2000a; Kamiya et al., 2001; Sanchez-Chapula et al., 2002)[, 50 μM propafenone blocked the other channels' tail currents much more than those of F656A (see Fig. 1). G628C/S631C (a double mutant that does not inactivate) was blocked by 85.9 ± 2.2% ($n = 5$), showing that inactivation is not obligatory for block by propafenone. The finding that propafenone block was only slightly altered by mutation of Tyr652 was particularly unexpected, because this residue also faces into the inner cavity of the channel, is located next to Phe656 (separated by one turn of the S6 α-helix), and has been shown to be critical for binding to nearly all other compounds investigated. Vesnarinone, the only other low-affinity blocker investigated in detail (Kamiya et al., 2001), also did not show a strong interaction with Tyr652. Kamiya et al. (2001) suggested that the reduced blockade potency of vesnarinone might be caused by the lack of a strong Tyr652 interaction combined with the lack of drug trapping (a result of vesnarinone's being uncharged). Propafenone is charged and does exhibit drug trapping, but it lacks the Tyr652 interaction, as does vesnarinone; this is concordant with its functional HERG blockade potency in *X. laevis* oocytes, in that propafenone falls between vesnarinone and the high-affinity blocking methanesulfonanilides. Overall, the features of propafenone blockade of HERG differ from those of vesnarinone, which was shown to have wide spectrum of molecular determinants in this region, including strong interactions with the residues at the base of the pore helix (Thr623, Ser624, Val625). Although the testing of the mutants selected does not exclude the possibility that additional binding interactions might occur between S5 residues or other S6 residues thought not to line the pore, our data reveal a distinct profile for propafenone with respect to those residues thus far considered to be important for drug-HERG interactions.

Drug Trapping of Propafenone. Experimental evidence suggested that drug trapping of propafenone by HERG occurred. First, unlike many other low-affinity HERG blockers [e.g., vesnarinone (Kamiya et al., 2001) and chloroquine (Sanchez-Chapula et al., 2002)], recovery from propafenone-mediated block did not occur while holding V_m at −90 mV (data not shown). However, unblock did occur if the drug was

TABLE 1
FlexiDock analysis of drug binding to HERG homology models
Binding-site normally defined as G648/S649/Y652/F656/S660 and all atoms within 4.5 Å. All side-chain bonds in binding site were allowed to rotate.

Drug	Channel State	Lowest Energy Score	Number of Runs	Number of Generations
Propafenone	Closed	−192	33	3,940,000
Propafenone	Open	−207	27	4,210,000
MK-499	Closed	−137	26	3,716,000
MK-499	Open	−198	11	1,140,000

washed off for several minutes *and* channels were subsequently opened by depolarization (Fig. 2). Thus, access to and escape from the inner cavity is dependent on opening of the activation gate. Second, there were no significant changes in any deactivation time constants when comparing currents in control and 3 μM propafenone containing solutions ($P > 0.30$ for t tests during deactivation at -140, -120, and -70 mV) after a steady-state level of activation induced by a 5-s step to 0 mV). Rapid recovery from block or unblock that results from channel deactivation often leads to a slowing of the current decay during channel deactivation (i.e., an apparent increase in deactivation time constant) because the activation gate is unable to close while drug is bound to the channel. These data suggest that propafenone does not exhibit a foot in the door block of HERG.

To determine whether or not propafenone becomes trapped within the inner cavity by closure of the activation gate, we used the D540K mutant of HERG, which can open upon hyperpolarization as well as upon depolarization (Sanguinetti and Xu, 1999). At the single channel level, the mechanism of the increased conductance of D540K is not associated with any change in single-channel conductance (Mitcheson et

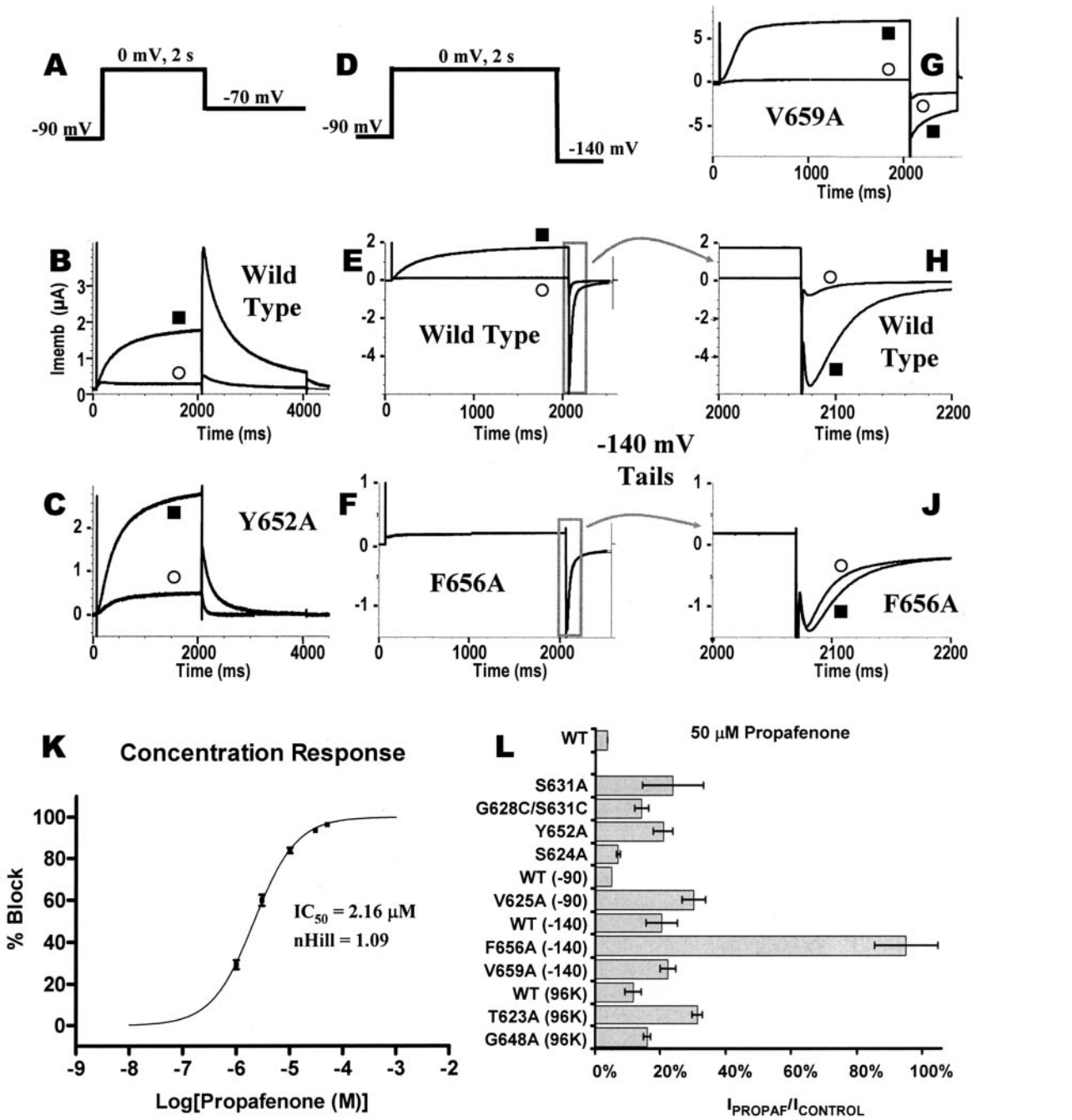

Fig. 1. Molecular determinants of blockade in the pore/S6 region. A–J, representative current traces for HERG and mutant HERG channels in the absence (■) and presence (○) of 50 μM propafenone. A shows the command voltage protocol for B and C, D shows the command protocol for E–J. H and J are the same as E and F, but with a close-up of the relevant time period. Ordinates are membrane current (I_{memb}) in microamperes. K, concentration-response curve for wild-type HERG peak tail currents in 2 mM K^+. L, summary of mean current remaining with 50 μM propafenone in all mutants tested. n = 3–5 for all.

al., 2000b) and is caused by destabilization of the closed state. This mutant channel allowed us to test whether having the channel in a conducting state while strongly directing the driving force for both K^+ ions and positively charged propafenone toward the cytosol was sufficient to relieve channel blockade. With D540K channels, repeated hyperpolarizing voltage commands led to channel opening and the diminution of the channel block in the presence of the methanesulfonanilide MK-499 (Mitcheson et al., 2000b), suggesting that the mechanism of the open-channel block was based on trapping of the drug inside the channel inner cavity during channel closure.

D540K-HERG was blocked by 3 μM propafenone when depolarizing pulses were applied. Rapid recovery from block (within 200 ms) could occur during a single hyperpolarizing pulse to −120 mV, even in the continued presence of drug. Such recovery did not occur with repolarization back to −70 or −40 mV (Fig. 3). The observation that hyperpolarization-dependent channel opening was critical for recovery was underscored by the fact that no recovery from block occurred with the D540A mutant (data not shown), which (like wild-type HERG) does not open with hyperpolarization. All these data support the idea that the mechanism of propafenone blockade of HERG involves drug trapping, with rapid on and off rates, and that after initial opening and commencement of blockade, propafenone can and probably does reside inside the inner cavity in the closed state; however, we cannot rule out that propafenone may interfere with channel closure, resulting in a configuration in which the propafenone-HERG inner cavity configuration is neither open nor closed (e.g., partially closed) and is yet functionally blocked. We propose that in the open-hyperpolarized state, the blockade of the channel by propafenone was compromised, perhaps because the Phe656 binding site (which may consist of side chains from more than one of the four Phe656 residues) is perturbed or inaccessible in this state.

To determine whether or not hyperpolarization per se (i.e., without maintaining a highly conducting state) was sufficient to relieve channel blockade, blockade was determined for fully activated wild-type HERG after increasing durations of deactivation at −120 mV (Fig. 4). The effect of hyperpolarization on recovery from block of wild-type HERG was assessed by stepping back to 0 mV and measuring the instantaneous component of current resulting from the increase in K^+ ion driving force at this potential. Currents were curve-fitted and extrapolated back to the beginning of the voltage step to give a measure of current availability.

In contrast to D540K-HERG, blockade of wild-type HERG by propafenone was not relieved at −120 mV between 20 and 120 ms (after 120 ms, currents were too small to compare), and block was not relieved in similar protocols when deactivation took place at −40 or −70 mV (Fig. 4). The lack of time-dependent recovery from blockade during deactivation is consistent with the hypothesis that propafenone was trapped in wild-type HERG; however, the lack of recovery between 20 and 120 ms suggests that there is a difference in

TABLE 2

Summary concentration response data

Summary of the concentration response data from wild-type HERG, F656A, Y652A, and V625A tail currents under the conditions listed. The fit of F656A block by propafenone resulted in an abnormally large Hill Slope (n_H), probably caused by fitting of only three points of the curve; higher concentrations were associated with solubility issues as explained in the text. By fixing the Hill slope to 1, the IC_{50} was found to be 246 μM. The Hill slope of V625A may be slightly less than 1 because of the effects of this mutation on the selectivity of the channel. CI, confidence interval.

Channel	Voltage Step	K^+	IC_{50}	IC_{50}	n_H	n_H
		mM	*μM*	*95% CI*		*95% CI*
Wild type	−70 mV	2	2.16	1.98 to 2.34	1.09	0.99 to 1.20
Wild type	−70 mV	96	4.38	3.76 to 5.11	0.94	0.81 to 1.07
F656A	−140 mV	2	205	83 to 506	1.86	−0.99 to 4.71
Y652A	−70 mV	2	13.6	8.2 to 22.4	1.25	0.49 to 2.00
V625A	−70 mV	2	12.1	6.8 to 21.5	0.63	0.32 to 0.94

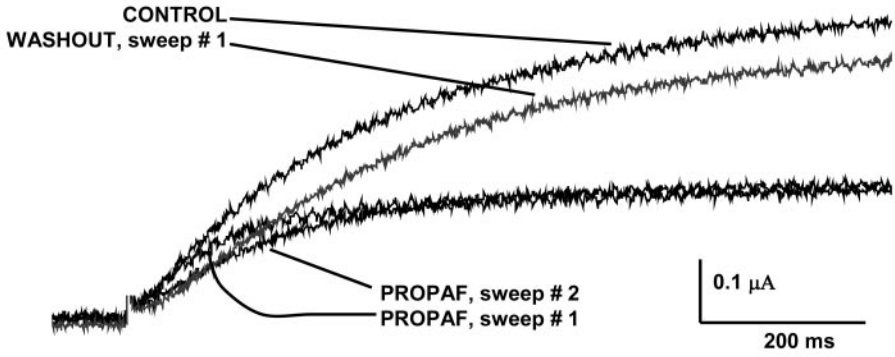

Fig. 2. Rapid onset and reversibility of block by propafenone. This figure shows the first second of representative current traces elicited by a depolarizing command protocol (depolarizing step to 0 mV for 5 s, followed by a repolarizing step to −120 mV for 1 s, interpulse interval 10 s) before drug addition, after 3 μM propafenone addition, and after washout of propafenone. After a steady HERG current baseline was established in control solution ("control"), propafenone-containing superfusate was washed on for 2 min to allow for complete fluid exchange while the oocyte remained at the holding potential (−90 mV). After four sweeps in propafenone (the first two of which are shown, PROPAF sweep 1 and PROPAF sweep 2), control superfusate was washed into the bath for 5 min while the voltage remained at the holding potential, and then the voltage command protocol was employed to elicit a final current (washout). Although the latter 700 ms of PROPAF sweeps 1 and 2 are nearly superimposed, the initial 100 ms of PROPAF sweep 1 is nearly identical to the control trace, whereas the initial 100 ms of PROPAF sweep 2 are nearly superimposed over the washout sweep 1 trace. Capacitative transients are blanked. Typical of five cells.

the propafenone binding site in the deactivating wild-type channel versus the OH (open hyperpolarized) state in the D540K channel. The differences in percentage block at −120 compared with −70 or −40 mV are relatively small, occur within the first 10 ms, and may be caused in part by differences in ionic flux through the pore. Although the wild-type channel does not release propafenone upon repolarization, the results for wild-type HERG and D540K suggest that channel opening is necessary (although not sufficient in the case of wild-type) for the drug to exit the channel. Thus, the mode of open-state blockade [as described previously (Duan et al., 1993; Mergenthaler et al., 2001; Paul et al., 2002)] involves drug trapping or another mechanism that holds the drug within the channel when the channel is closed.

Mutant Channels Do Not Release Propafenone Faster Than Wild-Type When Closed. The lack of reversible blockade while the channel is closed could be caused by drug trapping per se or could result from closed-state interactions with inner cavity residues. Such interactions would be difficult to measure directly using electrophysiological techniques, because the channels are in a nonconducting state. However, monitoring recovery from block after drug washout provides an indirect means of looking at drug binding affinity, because experimental interventions that lower binding affinity would speed up the kinetics of recovery from block and untrapping. Therefore, we compared wild-type channel recovery from block after drug washout at negative potentials with the same measurements from inner cavity mutants. To test the amount of blockade while minimizing the time spent in the open-state (thus optimizing the electrophysiological measurement of blockade of the closed-channel), a short depolarizing pulse (a 40-ms step to +40 mV) was used to open quickly the channels followed by a short repolarizing step (200 ms to −60 mV) to allow for the observation of the comparatively larger tail currents (the "sampling protocol"; see Fig. 5). Measurements of fractional blockade (normalized to the first sweep of the protocol) were made at a baseline in control solution (last sweep of the protocol before adding drug), in pseudo-steady-state blockade by 10 μM propafenone, and then in the first sweep after washout of the drug for 5 min—washout was performed while the holding potential was maintained at −120 mV to maintain channel

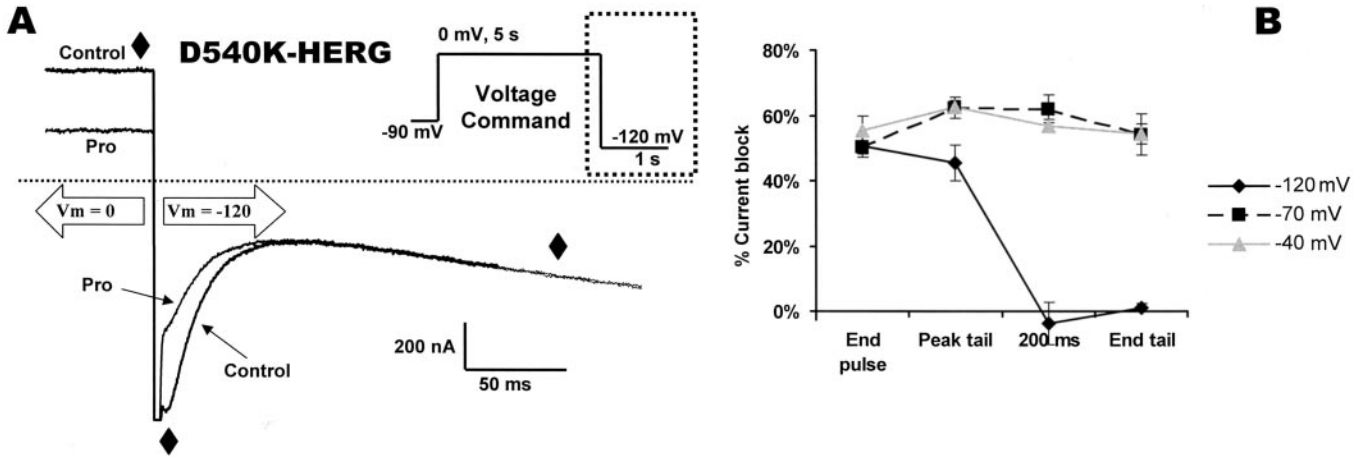

Fig. 3. Trapping and release of propafenone in D540K. To determine whether propafenone was trapped in the D540K channel, a protocol as in A (inset) was applied to the oocyte in the presence and absence of 3 μM propafenone. Two other similar protocols (differing only in the final repolarizing voltage) were also performed with the same cells. A shows segment (see dotted box in inset for the segment shown) of a representative pair of D540K current traces that are attenuated in the presence of propafenone during depolarization but during repolarization to −120 mV, drug blockade is eliminated. The diamonds indicate three of the four time points (left to right, end pulse, peak tail, 200 ms) at which analysis of mean currents were performed. The horizontal dotted line indicates zero current. B, the mean D540K block at different times during protocol in A (n = 5).

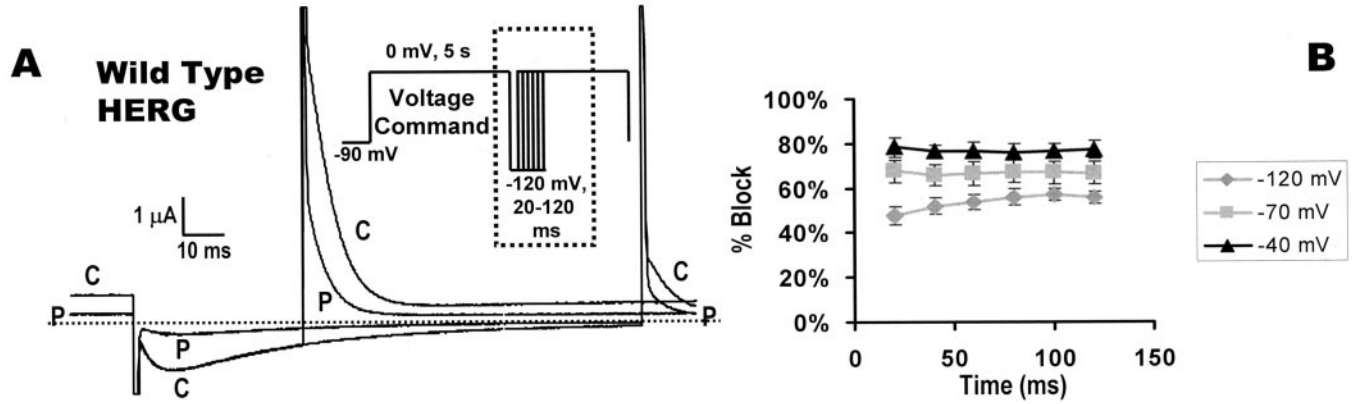

Fig. 4. Trapping of propafenone in wild-type HERG. The percentage blockade by 3 μM propafenone of wild-type HERG current was not reduced by the duration of repolarization at −120 mV. Potential was held at −90 mV, depolarized to 0 mV for 5 s, repolarized to −120 mV for increasing durations of time (20 to 120 ms in 20-ms steps), before depolarization to 0 mV (three-pulse protocol). Similar experiments were performed using voltages of −70 and −40 mV. A shows a representative series of traces for −120 mV deactivation steps, showing only the sweeps for time points at 40 and 120 ms for clarity (C = control, P = 3 μM propafenone). B, the percentage block was calculated for each duration of repolarization. n = 5 for all.

closure. An identical series of experiments was then performed on the same oocyte but with only a 30-s washout. The measured currents for each oocyte were nearly identical for the experiments involving the 5-min versus the 30-s washout (Fig. 5C). If two variables are identical, then a regression of one on the other should result in a zero intercept and a slope of unity. A linear regression of fractional blockade values for the 5-min washout data on those for the 30-s washout data (e.g., the sweeps in Fig. 5, Ai and B) had a slope that was not significantly different from 1 (0.9949, 95% confidence interval = 0.9236 to 1.0663, $P = 0.872$) and had a y-intercept that was not significantly different from 0 (0.0038, 95% confidence interval = −0.0187 to 0.0263, $P = 0.701$, and for the entire model, $R^2 = 0.9936$). This result suggests that the recovery from blockade is effectively independent of the time spent in the closed state compared with the level of recovery from blockade that occurs in only 40 ms in the open state. This rapid recovery from blockade during an initial opening of the channel can be seen in Fig. 5, A and B, in the washout sweeps, which show an increasing tail current (rather than a tail current peak) that is reminiscent of the cross-over currents associated with a "foot in the door" type of blockade; this cross-over current is only observed with propafenone immediately after the drug has been washed out (and the drug's concentration gradient would be out of the channel), whereas true "foot-in-the-door" blockade current cross-over occurs with the drug present in the superfusate. Thus, recovery from blockade after washout of propafenone is very rapid

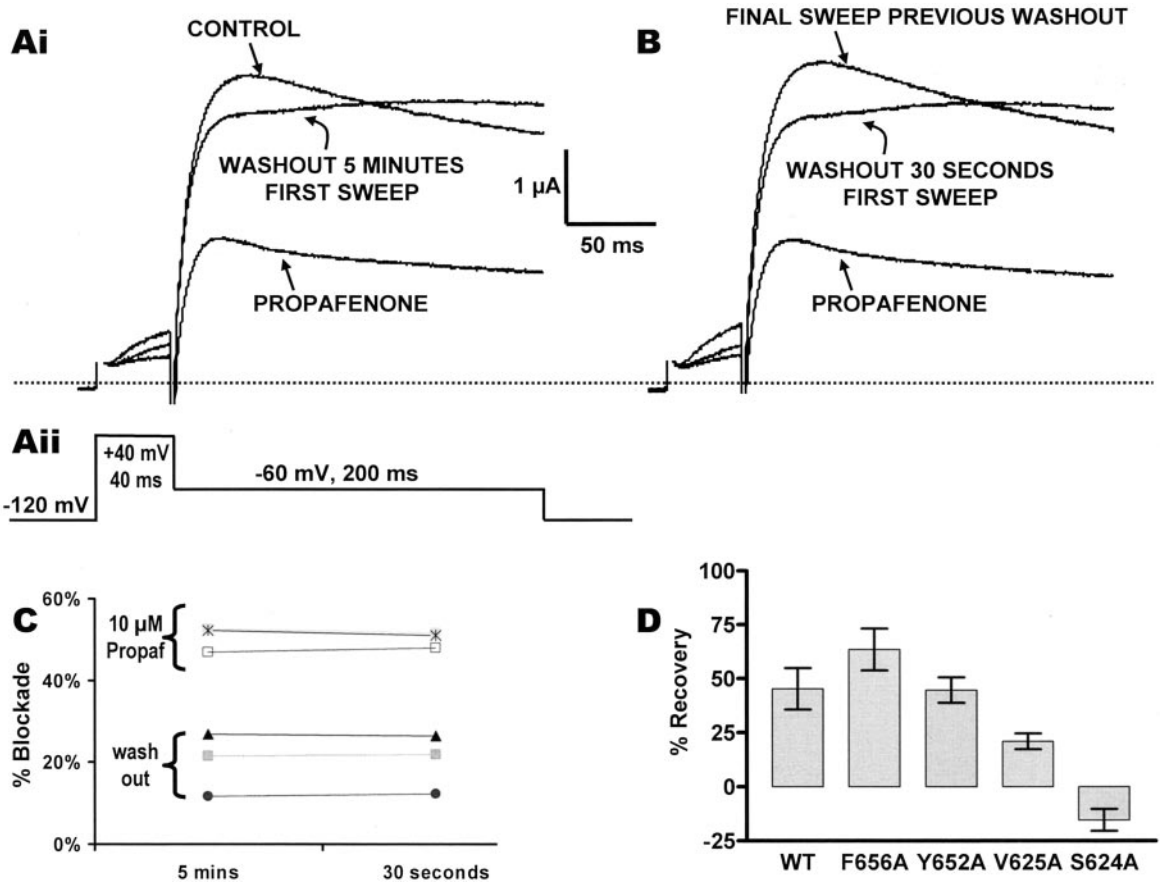

Fig. 5. Reversibility of block while the channels are closed. The reversibility of wild-type HERG blockade was compared in the same oocytes after a 5-min period of washout and after a 30-s period of washout; representative traces all from the same oocyte are shown in Ai and B. Because functional blockade cannot be measured electrophysiologically except during the open state, a blockade "sampling protocol" was employed (Aii) in which the membranes were strongly depolarized but for a minimal time (40 ms) to maximize tail currents while minimizing time in the open state when propafenone could exit from a trapped condition. To maintain a definitive closed state, all experiments in Fig. 5 involved a holding potential of −120 mV; blockade was determined for the peak of the tail current elicited at −60 mV. At first, the oocytes were tested with the sampling protocol while they were superfused with control superfusate (control, Ai) and then were superfused with 10 μM propafenone for 1 min while held at −120 mV. Pseudo-steady-state blockade was elicited by depolarizing the membrane to 0 mV for 2 s followed by 2 s at −70 mV (i.e., a single sweep similar to Fig. 1A), and then blockade was measured using the sampling protocol (Ai, propafenone, only two sweeps were allowed). Then, while the cell membrane potential was held at −120 mV, washout of propafenone was effected by superfusion of control solution for 5 min. The sampling protocol was applied again; the amount of block was calculated isochronally with the peak of the control current sweep. Then, while superfusing control solution, the sampling protocol was applied repeatedly for 5 min (start-to-start interval, 10 s), which was sufficient for a steady-state baseline to be re-established (B, final sweep previous washout). The pseudo-steady-state blockade by propafenone (B, propafenone) followed by washout was repeated as above, except that washout was allowed to proceed for only 30 s at −120 mV before applying the sampling protocol (B, washout 30 s first sweep). C shows the data for wild-type HERG, demonstrating that the percentage blockade is the same with each application of drug, and that recovery from block is identical after 5 min or 30 s of washout (e.g., Ai versus B). Paired symbols connected by a line represent an individual oocyte. $n = 3$ oocytes. A similar series of experiments was performed for wild-type (WT) and a selection of mutant channels for the 5-min washout period (D). F656A tail currents were measured at −140 mV, and the short depolarization to +40 mV was slightly longer (60 ms) in duration for S624A to compensate for slower activation kinetics. The concentration of propafenone used for each mutant was chosen to elicit a fractional blockade of ~50% (wild-type, 10 μM; F656A, 300 μM; Y652A, 30 μM; V625A, 30 μM; and S624A, 10 μM). $n = 3$ to 6 for all.

when the wild-type channels are open (> 50% recovery in less than 10 ms) and is virtually undetectable in the time scale tested (5 min) when the channels are held closed.

Even though recovery from propafenone blockade of the wild-type channel is extremely slow when the channel is in the closed state, it is possible to test whether the mutations tested (particularly F656A) cause a change in the level of recovery from blockade when the channel is held in the closed state (−120 mV). This was done for a selection of mutant HERG channels in a manner similar to that shown in Fig. 5Ai, in which the mutant channels were exposed to a level of propafenone that would elicit a fractional block of ~50%, and then the propafenone was washed off for 5 min (Fig. 5D); the varying concentrations of propafenone are necessary to establish comparable initial levels of blockade and is useful because recovery from blockade after the drug-containing superfusate has been replaced by control solution should depend on the level of blockade but be independent of the previous concentration of drug. Recovery from propafenone block of Tyr652, V625A and S624A was similar to or slower than that of wild-type HERG. Only F656A showed a quickening of recovery from block, although it was not significantly different from wild-type ($P > 0.05$). One-way analysis of variance with post hoc Bonferroni multiple comparison tests showed that the percentage recovery after 5 min of washout for the various mutant channels was different after similar levels of blockade by propafenone ($P = 0.0002$). This difference was individually statistically significant for wild-type versus S624A, Y652A versus S624A, F656A versus S624A, and F656A versus V625A ($P < 0.01$ for all). S624A has the unanticipated reverse effect on the wild-type channel of slowing the reversibility of blockade. This same mutation leads to an increased reversibility of blockade by the chlorobenzene derivative clofilium, presumably because of the interaction of the halogen of clofilium with this region of the HERG structure (Perry et al., 2004); an analogous halogen is absent from propafenone. These experiments suggest that none of the mutations tested significantly reduces propafenone's interaction with the channel in the closed state, although it does not exclude the possibility that F656A may have a small effect in that way.

Voltage-Dependent Mechanism of Blockade Predicted from Homology Models. The mechanism of HERG blockade by propafenone has been previously demonstrated to be voltage-dependent (Mergenthaler et al., 2001; Paul et al., 2002; Arias et al., 2003). Given that our data suggest that propafenone can interact with the residues of the inner cavity (as predicted by previous models based on the KcsA closed-channel structure), but primarily only at Phe656, it is possible that the voltage-dependence may be caused by gating-dependent effects on accessibility or spatial positioning of the Phe656 side chains for drug interactions. To test the latter possibility, we studied docking of propafenone into closed- and open-state homology models of the HERG pore region using the crystal structure co-ordinates of KcsA (closed channel) and MthK (open channel) as templates (Doyle et al., 1998; Jiang et al., 2002). The homologies are shown in Fig. 6, and the resulting models are shown in Fig. 7, A and B. Analysis of docking interactions with homology models cannot give unequivocal answers about the nature of the drug binding. Nevertheless, multiple FlexiDock runs of MK-499 in the closed-channel model resulted in a relatively small set of low-energy structures in which the drug adopted a reproducible conformation (data not shown) and made a well defined set of interactions with HERG residues facing the channel inner cavity (similar to those found by Mitcheson et al., 2000a). This differed for propafenone, in which FlexiDock located a large variety of different low-energy structures for the interaction with either open- or closed-channel models, although these were found to cluster in terms of their dominant interactions.

Inspection of docking to open- and closed-channel homology models suggests that the mutagenesis data for propafenone-mediated blockade might best be rationalized by interactions with the open-channel model. The "splaying out" of the terminal regions of the pore-lining helices in the open-channel model (Fig. 7B) renders the Phe656 side chains highly accessible to molecules approaching the channel from the cytoplasmic side of the membrane (the Cα − Cα separation across the pore at the level of Phe656 in the open-channel model is around 20 Å). A significant preference for interactions involving Phe656 over Tyr652 was observed in docking of propafenone to the open-channel model. Both aromatic rings of propafenone can make simultaneous π-stacking interactions with aromatic rings of Phe656 on adjacent, or opposite, channel subunits. Using a variety of initial conditions, FlexiDock was able to find several different low-energy conformations, and almost all of the lowest energy structures of propafenone involved simultaneous π-stacking interactions of propafenone's aromatic rings with adjacent aromatic rings of two Phe656 residues (the lowest energy structure is shown in Fig. 7, B and D).

As with the open-channel model, the interactions of propafenone with HERG residues in the inner cavity of the closed-channel model were promiscuous, and a variety of different low-energy conformations and interactions were found. Nevertheless, in all starting positions and configura-

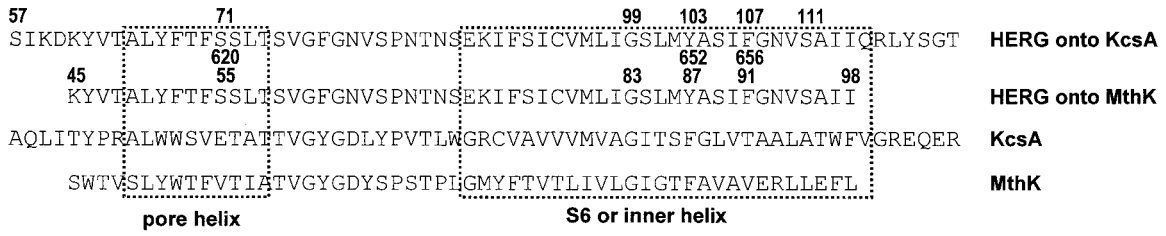

Fig. 6. Sequence homologies used in constructing HERG closed- and open-state homology models. Sequences are annotated according to the location in the structural element of the channel. The top two lines are the sequences of HERG built onto the closed-state channel structure of KcsA (according to the homology with the KcsA sequence in line 3) and onto the open-state channel structure of MthK (according to the homology with the MthK sequence in line 4). The numbers above the HERG sequences are the sequence numbers of KcsA or MthK that become transferred onto the HERG homology models. The HERG amino acid sequence numbers are shown in larger font below the HERG/KcsA alignment (i.e., Tyr652 of HERG aligns with Phe103 of KcsA and Phe87 of MthK).

tions of both stereoisomers of propafenone in the closed-channel model, the lowest energy binding interactions were achieved only on movement of the drug into the inner cavity below the selectivity filter (the lowest energy structure is shown in Fig. 7, A and C). Furthermore, in the closed-channel model, the channel is constricted in the region of Phe656 ($C\alpha - C\alpha$ distance across the pore is 10 Å), and there is simply not enough space for propafenone to make simultaneous π-stacking interactions with Phe656 side chains involving both of propafenone's aromatic rings (Fig. 7, E and F).

A summary of all the FlexiDock runs, for both open- and closed-channel models, is shown in Fig. 8. In open-state models, a cluster of low-energy docking structures was obtained in which nearly or fully exclusive interactions between

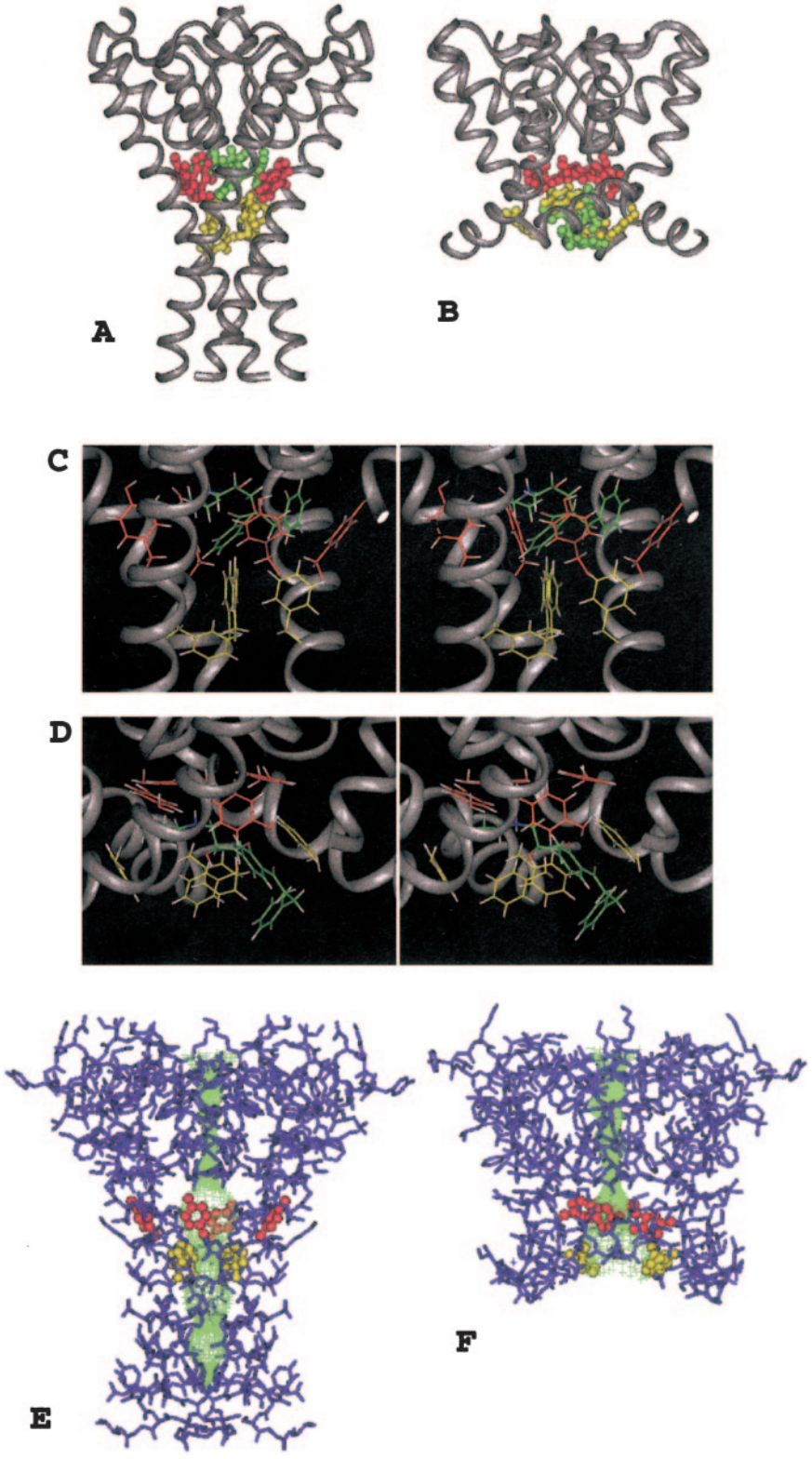

Fig. 7. Modeled docking of propafenone. Lowest score structures of propafenone docked into closed- (A) and open-state (B) homology models (extracellular surface at top); C and D are stereo views of the propafenone binding site in closed- and open-state models, respectively. Tyr652 (red) and Phe656 (yellow) side chains are displayed along with backbone ribbons (gray). Propafenone carbons are green. E and F show line diagrams of the atomic coordinates of the closed (left) and open (right) HERG homology models; the accessible channel pore regions, determined using HOLE (Smart et al., 1996), are stippled green. The side chains of Tyr652 (red) and Phe656 (yellow) are shown with solid rendering. Note that in the closed-channel model, the inner cavity is constricted at the level of Phe656 and as such would prevent simultaneous π stacking interactions between the two aromatic rings of propafenone and two of the Phe656 residues.

propafenone and Phe656 side chains were obtained. In closed-state models, no low-energy structures were obtained that had exclusive propafenone-Phe656 π:π interactions. In most low-energy structures from the closed-channel model, mixed interactions of propafenone with both Phe656 and Tyr652 aromatic rings were found. These generally corresponded to the migration of propafenone into the inner cavity below the selectivity filter. A number of runs in which propafenone was constrained to interact with the closed model at the level of the Phe656 residues resulted in very poor energies (these correspond to the grouping of runs with high propafenone-Phe656 and zero or near-zero propafenone-Tyr652 interactions). Thus, only in open-channel models were exclusive interactions with Phe656 (rather than Tyr652) side chains reproducibly found. The conformational lability of propafenone, and its ability to make a range of different interactions with Phe656 residues in the modeling by FlexiDock, may be a reflection of the low-affinity of the drug with HERG. The failure of modeling the closed-channel's interaction with propafenone to provide a consistent low-energy conformation that was concordant with the observed mutagenesis data may indicate that the interactions between propafenone and the closed channel are weaker than the interactions with the open channel. Furthermore, it suggests that the main blocking criterion in the closed channel may be spatial restriction caused by the ring of the four Phe656 side chains (which are closer together in the closed-state model than in the open-state model) that prevents egress of the propafenone molecule from the channel's inner cavity. This further supports the proposition that the voltage-dependent blocking mechanism includes drug trapping.

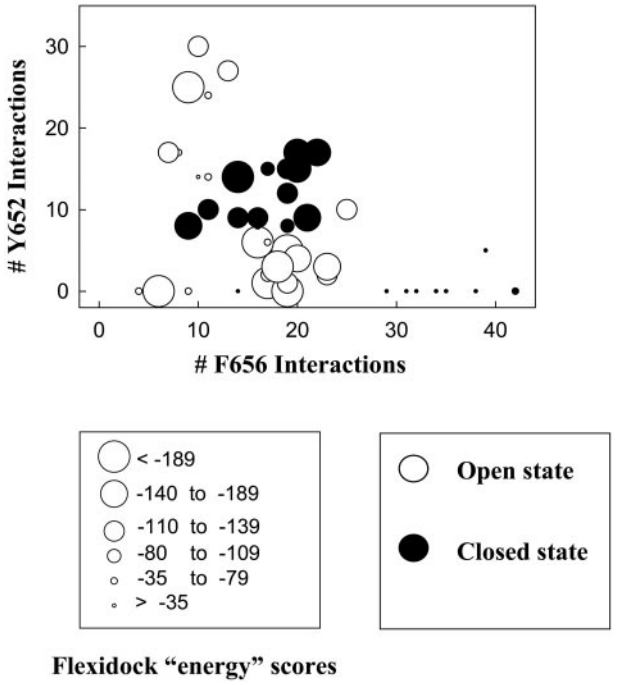

Fig. 8. Aromatic ring interactions between the drug and HERG models. Propafenone docking to open-state (○) and closed-state (●) HERG homology models was characterized in terms of aromatic ring (π:π) interactions. Each docking run was ranked by energy (see key at bottom) and defined by the number of HERG Tyr652 or Phe656 aromatic ring atoms within 4.5 Å of a propafenone aromatic ring atom. A distance cutoff of 4.5 Å was taken to be the maximum separation of aromatic ring atoms that give rise to energetically favorable π-stacking interactions (McGaughey et al., 1998; Chelli et al., 2002). The maximum number of ring atoms per Tyr652 or Phe656 was taken to be 11 (all ring carbons and ring-bound atoms *ortho*-, *meta*-, or *para*- to the carbon atom linking the ring to the β carbon of the side chain). Thus, a docking run in which all four Tyr652 (or Phe656) residues made maximum interactions with propafenone aromatic rings would have a value of 44, and a value of 10 to 11 corresponds to approximately 1 (parallel) π-stacking interaction between propafenone and the HERG model. Outliers in the closed-state model represent conformations in which the binding site was constrained to be Phe656, Ser660, and all atoms within 4.5 Å (i.e., excluding Tyr652); in these cases, FlexiDock could not locate a low-energy binding state. A few low-energy open-state docking results were found with significant Tyr652 interactions (outliers in the top left corner of the figure) but these conformers also made significant additional contacts with Phe656. The large majority of runs with the open channel found low-energy binding states exhibiting a large number of propafenone interactions with Phe656, and these were the only set of binding modes in either open- or closed-channel models that were consistent with the mutagenesis data described above.

Discussion

This study demonstrates that of the inner cavity residues known to be molecular determinants of pharmacological blockade of HERG, Phe656 is the most important one for propafenone blockade. We propose that the binding of propafenone to HERG is defined by interactions with an open-channel state (inactivation is not required) in which the Phe656 side chains are accessible and form the principal binding site. On channel closure, the drug is held or trapped in the inner cavity. Because there is no time-dependent recovery from blockade in the wild-type channel during current deactivation, rapid reversibility of blockade with the next depolarization may depend upon events occurring after closure of the channel. One possible sequence of events consistent with our results would be 1) channel closure and drug trapping accompanied by 2) release of the drug from Phe656-binding site into the inner cavity, followed by 3) drug release from the inner cavity after subsequent re-activation.

The structural models predicted that spatial restrictions near Phe656 could not maintain propafenone in the Phe656-bound (and presumably blocking) conformation in a KcsA-based closed-channel model, and that these spatial restrictions were responsible for trapping the drug in the inner cavity of the channel during long closures. In closed-channel homology models, the pore is constricted at the level of the Phe656 residues (Cα − Cα separation across the pore is 10 Å), and there is insufficient space to accommodate propafenone in configurations that allow exclusive interactions only with Phe656 side chains. Although there is ample room in the inner cavity for trapping of propafenone, all low-energy binding modes involved significant interactions with Tyr652 (Fig. 7, A and C). Thus, agreement between the mutagenesis and docking data were only obtained in the open-state model, where nearly exclusive interactions of propafenone with Phe656 were obtained (Fig. 8). It would seem that the Tyr652-propafenone interactions in the closed-channel model are not as energetically favorable as Phe656-propafenone interactions once the channel has opened. These results indicate a real and significant difference between HERG's interaction with propafenone versus its interactions with high-affinity blockers such as MK-499; indeed, we found low-energy docking modes of MK-499 with the closed-channel model that were both fully consistent with mutagenesis data and very similar to those previously obtained in an independent computational docking analysis (Mitcheson et al., 2000a).

Although the data presented here support the interaction

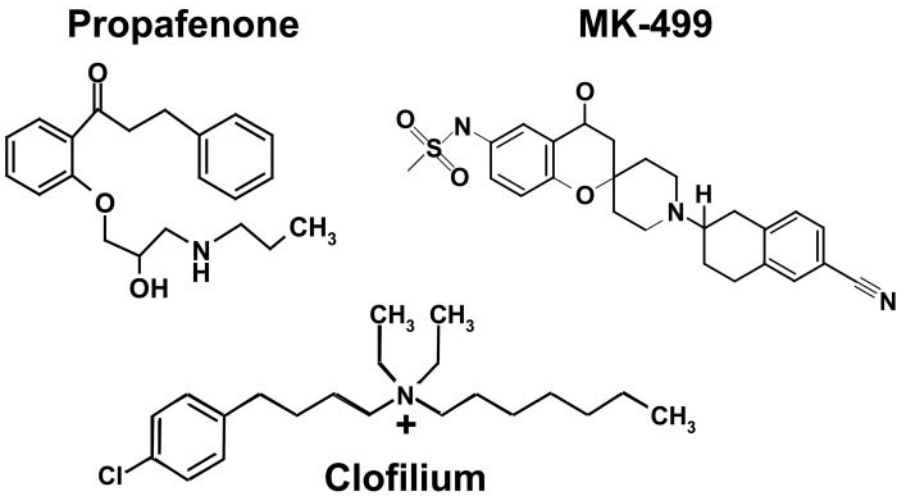

Fig. 9. Structural formulae of propafenone, MK-499, and clofilium.

of propafenone with the open state and do not support strong interaction with the closed state, the situation regarding the inactivated state(s) also warrants consideration. One study of propafenone's block of wild-type HERG (Arias et al., 2003) concluded that HERG might have a higher affinity for propafenone in the inactivated (rather than the open) channel state. However, in the present study, two noninactivating mutants (S631A and S628C/S631C) were effectively blocked by propafenone, indicating that channel inactivation is not obligatory for blockade to occur [compare with class Ia antiarrhythmic HERG blockers disopyramide (Paul et al., 2001), quinidine (Lees-Miller et al., 2000), and procainamide (Ridley et al., 2003)]. This does not exclude some affinity of HERG for propafenone in the inactivated state, so long as the affinity in the inactivated state is quantitatively similar in level to the open-state affinity.

Mergenthaler et al. (2001) suggested that propafenone acts on HERG from the cytoplasmic side of the membrane and binds to a site part of the way across the transmembrane electric field. They found that block was substantially reduced by lowering the pH of the extracellular solution to 6. The pK_a of propafenone is 8.8, suggesting that at pH 7.4, it is ~96% protonated, and at pH 6, it is ~99.8% protonated; thus, at acid pH, it would be predicted that propafenone would be less able to gain access to the cytosolic surface of the channel because of decreased membrane permeability. They also found that block increased continuously at progressively depolarized potentials (even at potentials above which the increase in open probability was only slight) and calculated that propafenone bound to a site with a fractional electrical distance $\delta = 0.2$ across the electric field. Other Woodhull analyses have also been performed that collectively suggest that propafenone senses between 9 and 27% of the transmembrane field measured from the interior (Mergenthaler et al., 2001; Paul et al., 2002; Arias et al., 2003). Thus, the drug's binding site is part of the way across the transmembrane electrical field, nearer to the cytoplasmic side of membrane. This is consistent with the fact that Phe656 is presumed to be located toward the cytoplasmic end of the pore inner cavity and that F656A was the only one of the mutants tested in which blockade by 50 μM propafenone was dramatically attenuated.

The mechanism of recovery from block by propafenone is probably not caused by a voltage-dependent process such as 'knock off' by K^+ influx at hyperpolarized potentials, because high extracellular K^+ had only a small change on IC_{50} and recovery from block. Blockade of the wild-type channel during repolarization/deactivation was not time-dependent (at least not within the range of 20–120 ms) but did show some voltage dependence (Fig. 4); this suggests that recovery from block was unlikely to be related to voltage dependence of channel deactivation but resulted instead from an action of the electric field on drug binding. Thus, our data are concordant with the notion that the electric field may act directly on the drug molecule and can drive propafenone out of the channel inner cavity (i.e., toward the cytoplasm) so long as the channel is open when the membrane is hyperpolarized.

The Potency of Propafenone Blockade of HERG. Based on previous studies of the molecular determinants of HERG pharmacology, we and others have postulated that π-stacking between aromatic groups of the drug and Phe656 and Tyr652 of HERG are important for high-affinity binding (Lees-Miller et al., 2000; Mitcheson et al., 2000a). Fernandez et al. (2004) have recently demonstrated that the potency for block by MK-499, cisapride, and terfenadine was well correlated with measures of hydrophobicity at position 656, especially the two-dimensional approximation of the van der Waals hydrophobic surface area of the side chain of the residue. For residue 652, an aromatic side group was essential for high-affinity block, suggesting the importance of a cation-π interaction between Tyr652 and the basic tertiary nitrogen of these drugs. Concordant with this, propafenone only weakly interacts with Tyr652, and its potency for blockade is also found to be lower than methanesulfonanilides. Pharmacophore models predict that important features of potent HERG channel blockers are 1) a basic nitrogen that is usually protonated at physiological pH and 2) three hydrophobic centers of mass (centroids) arranged in a specific spatial pattern around the centrally located nitrogen (Cavalli et al., 2002; Ekins et al., 2002). For many potent HERG blockers, these centroids are aromatic groups. Propafenone does not have this many aromatic groups, the nitrogen is not centrally located, and the arrangement of these groups is more flexible than in high-affinity HERG blockers such as MK-499 (see Fig. 9).

We found that the IC_{50} for propafenone blockade of heterologous HERG expressed in *X. laevis* oocytes was 2.16 μM (Table 2), which is 5-fold larger than the IC_{50} we have observed previously in mammalian cells expressing HERG (Paul et al., 2002); the greater potency of drug block in

mammalian cells compared with oocytes is a common finding and may be related to the lipophilic yolk sac in oocytes that acts to sequester the drug. Our IC_{50} of 2.16 μM is 7-fold lower than the potency determined by Mergenthaler et al. (2001), who also used *X. laevis* oocytes. The reason for the difference in IC_{50} between their study and our own is not clear, but it may result from differences in recording conditions and from the reduced contamination by endogenous currents in the present study.

Conclusions

We have investigated the molecular determinants of HERG blockade by propafenone, a clinically important class Ic antiarrhythmic agent. Our results show for the first time that propafenone is retained in the channel because of gating upon repolarization. This may have important implications for rapid onset of I_{Kr} block during cardiac action potentials because it ensures that the drug remains close to its receptor. The mutagenesis studies suggest that, of all HERG residues previously shown to mediate drug blockade, Phe656 is the only residue facing into the cavity with a role in propafenone binding; however, we cannot exclude the possibility that propafenone has additional interactions with residues in S5 or S6 that have not previously been shown to be determinants of drug blockade of HERG. Furthermore, docking simulations using computer models of both the open- and closed-channel suggest that propafenone can only make exclusive interactions with Phe656 in the open state. Our results additionally support the idea that, at the molecular level, analysis of binding of HERG blockers should consider both open- and closed-channel states and that this may be particularly relevant for low-affinity blockers. Finally, we conclude that the accessibility of the Phe656 residues forming the binding site to drugs in the inner cavity changes between the open and closed states.

Acknowledgments

We gratefully acknowledge technical support from Kate Metcalfe and Seung Ho Kang, computational support from Peter Dickens, and guidance from James Walsh and James Stelfox.

References

Arias C, Gonzalez T, Moreno I, Caballero R, Delpon E, Tamargo J, and Valenzuela C (2003) Effects of propafenone and its main metabolite, 5-hydroxypropafenone, on HERG channels. *Cardiovasc Res* **57:**660–669.

Cavalli A, Poluzzi E, De Ponti F, and Recanatini M (2002) Toward a pharmacophore for drugs inducing the long QT syndrome: insights from a CoMFA study of HERG K^+ channel blockers. *J Med Chem* **45:**3844–3853.

Chelli R, Gervasio FL, Procacci P, and Schettino V (2002) Stacking and T-shape competition in aromatic-aromatic amino acid interactions. *J Am Chem Soc* **124:** 6133–6143.

Delpon E, Valenzuela C, Perez O, Casis O, and Tamargo J (1995) Propafenone preferentially blocks the rapidly activating component of delayed rectifier K current in guinea pig ventricular myocytes. *Circ Res* **76:**223–235.

Doyle DA, Morais Cabral JH, Pfuetzner RA, Kuo A, Gulbis JM, Cohen SL, Chait BT, and Mackinnon R (1998) The structure of the potassium channel: molecular basis of K^+ conduction and selectivity. *Science (Wash DC)* **280:**69–77.

Duan D, Fermini B, and Nattel S (1993) Potassium channel blocking properties of propafenone in rabbit atrial myocytes. *J Pharmacol Exp Ther* **264:**1113–1123.

Ekins S, Crumb WJ, Sarazan RD, Wikel JH, and Wrighton SA (2002) Three-dimensional quantitative structure-activity relationship for inhibition of human ether-a-go-go-related gene potassium channel. *J Pharmacol Exp Ther* **301:**427–434.

Fernandez D, Ghanta A, Kauffman GW, and Sanguinetti MC (2004) Physicochemical features of the HERG channel drug binding site. *J Biol Chem* **279:**10120–10127.

Funck-Brentano C, Kroemer HK, Lee JT, and Roden DM (1990) Propafenone. *N Engl J Med* **322:**518–525.

Gessner G, Zacharias M, Bechstedt S, Schonherr R, and Heinemann SH (2004) Molecular determinants for high-affinity block of human EAG potassium channels by antiarrhythmic agents. *Mol Pharmacol* **65:**1120–1129.

Hii JT, Wyse DG, Gillis AM, Cohen JM, and Mitchell LB (1991) Propafenone-induced torsade de pointes: cross-reactivity with quinidine. *Pacing Clin Electrophysiol* **14:**1568–1570.

Ishii K, Kondo K, Takahashi M, Kimura M, and Endoh M (2001) An amino acid residue whose change by mutation affects drug binding to the HERG Channel. *FEBS Lett* **506:**191–195.

Jiang Y, Lee A, Chen J, Cadene M, Chait BT, and Mackinnon R (2002) Crystal structure and mechanism of a calcium-gated potassium channel. *Nature (Lond)* **417:**515–522.

Kamiya K, Mitcheson JS, Yasui K, Kodama I, and Sanguinetti MC (2001) Open channel block of HERG K^+ channels by vesnarinone. *Mol Pharmacol* **60:**244–253.

Lees-Miller JP, Duan Y, Teng GQ, and Duff HJ (2000) Molecular determinant of high-affinity dofetilide binding to HERG1 expressed in *Xenopus* oocytes: involvement of S6 sites. *Mol Pharmacol* **57:**367–374.

Levi AJ, Hancox JC, Howarth FC, Croker J, and Vinnicombe J (1996) A method for making rapid changes of superfusate whilst maintaining temperature at 37 degrees C. *Pflueg Arch Eur J Physiol* **432:**930–937.

McGaughey GB, Gagné M, and Rappé AK (1998) π-Stacking interactions. alive and well in proteins. *J Biol Chem* **273:**15458–15463.

Mergenthaler J, Haverkamp W, Huttenhofer A, Skryabin BV, Musshoff U, Borggrefe M, Speckmann EJ, Breithardt G, and Madeja M (2001) Blocking effects of the antiarrhythmic drug propafenone on the HERG potassium channel. *Naunyn Schmiedeberg's Arch Pharmacol* **363:**472–480.

Milnes JT, Crociani O, Arcangeli A, Hancox JC, and Witchel HJ (2003) Blockade of HERG potassium currents by fluvoxamine: incomplete attenuation by S6 mutations at F656 or Y652. *Br J Pharmacol* **139:**887–898.

Mitcheson JS, Chen J, Lin M, Culberson C, and Sanguinetti MC (2000a) A structural basis for drug-induced long QT syndrome. *Proc Natl Acad Sci USA* **97:**12329–12333.

Mitcheson JS, Chen J, and Sanguinetti MC (2000b) Trapping of a methanesulfonanilide by closure of the HERG potassium channel activation gate. *J Gen Physiol* **115:**229–240.

Paul A, Witchel HJ, and Hancox JC (2001) Inhibition of HERG potassium channel current by the class 1a antiarrhythmic agent disopyramide. *Biochem Biophys Res Commun* **280:**1243–1250.

Paul AA, Witchel HJ, and Hancox JC (2002) Inhibition of the current of heterologously expressed HERG potassium channels by flecainide and comparison with quinidine, propafenone and lignocaine. *Br J Pharmacol* **136:**717–729.

Perry M, De Groot MJ, Helliwell R, Leishman D, Tristani-Firouzi M, Sanguinetti MC, and Mitcheson JS (2004) Structural determinants of HERG channel block by clofilium and ibutilide. *Mol Pharmacol* **66:**240–249.

Rehnqvist N, Ericsson CG, Eriksson S, Olsson G, and Svensson G (1984) Comparative investigation of the antiarrhythmic effect of propafenone (Rhythmonorm) and lidocaine in patients with ventricular arrhythmias during acute myocardial infarction. *Acta Med Scand* **216:**525–530.

Ridley JM, Milnes JT, Benest AV, Masters JD, Witchel HJ, and Hancox JC (2003) Characterisation of recombinant HERG K^+ channel blockade by the class Ia antiarrhythmic drug procainamide. *Biochem Biophys Res Commun* **306:**388–393.

Roden DM, Lazzara R, Rosen M, Schwartz PJ, Towbin J, and Vincent GM (1996) Multiple mechanisms in the long-QT syndrome. Current knowledge, gaps and future directions. The SADS Foundation Task Force on LQTS. *Circulation* **94:** 1996–2012.

Sanchez-Chapula JA, Navarro-Polanco RA, Culberson C, Chen J, and Sanguinetti MC (2002) Molecular determinants of voltage-dependent human *ether-a-go-go* related gene (HERG) K^+ channel block. *J Biol Chem* **277:**23587–23595.

Sanguinetti MC, Jiang C, Curran ME, and Keating MT (1995) A mechanistic link between an inherited and an acquired cardiac arrhythmia: HERG encodes the I_{Kr} potassium channel. *Cell* **81:**299–307.

Sanguinetti MC and Xu QP (1999) Mutations of the S4–S5 linker alter activation properties of HERG potassium channels expressed in *Xenopus* oocytes. *J Physiol (Lond)* **514:**667–675.

Smart OS, Neduvelil JG, Wang X, Wallace BA, and Sansom MS (1996) HOLE: a program for the analysis of the pore dimensions of ion channel structural models. *J Mol Graph* **14:**354–360.

Spector PS, Curran ME, Keating MT, and Sanguinetti MC (1996) Class III antiarrhythmic drugs block HERG, a human cardiac delayed rectifier K^+ channel. Open-channel block by methanesulfonanilides. *Circ Res* **78:**499–503.

Address correspondence to: Harry J. Witchel, Cardiovascular Research Laboratories and Department of Physiology, School of Medical Sciences, University of Bristol, Bristol, BS8 1TD, UK. E-mail: harry.witchel@bristol.ac.uk